Environmental Science & Technology

Article

pubs.acs.org/est

Influence of Partial Denitrification and Mixotrophic Growth of NOB on Microbial Distribution in Aerobic Granular Sludge

Mari-K. H. Winkler,[†,‡,§] Quan H. Le,[†,§] and Eveline I. P. Volcke*[,†]

[†]Department of Biosystems Engineering, Ghent University, Coupure links 653, 9000 Gent, Belgium

[‡]Department of Civil and Environmental Engineering, University of Washington, Seattle, Washington 98195-2700, United States

Supporting Information

ABSTRACT: In aerobic granular sludge (AGS), the growth of nitrite oxidizing bacteria (NOB) can be uncoupled from the nitrite supply of ammonia oxidizing bacteria (AOB). Besides, unlike for conventional activated sludge, *Nitrobacter* was found to be the dominant NOB and not *Nitrospira*. To explain these experimental observations, two possible pathways have been put forward in literature. The first one involves the availability of additional nitrite from partial denitrification (nitrite-loop) and the second one consists of mixotrophic growth of *Nitrobacter* in the presence of acetate (ping-pong). In this contribution, mathematical models were set up to assess the possibility of these pathways to explain the reported observations. Simulation results revealed that both pathways influenced the nitrifier distribution in the granules. The nitrite-loop pathway led to an elevated NOB/AOB ratio, while mixotrophic growth of *Nitrobacter* guaranteed their predominance among the NOB population. Besides, mixotrophic growth of *Nitrobacter* could lead to NO emission from AGS. An increasing temperature and/or a decreasing oxygen concentration led to an elevated NOB/AOB ratio and increased NO emissions.

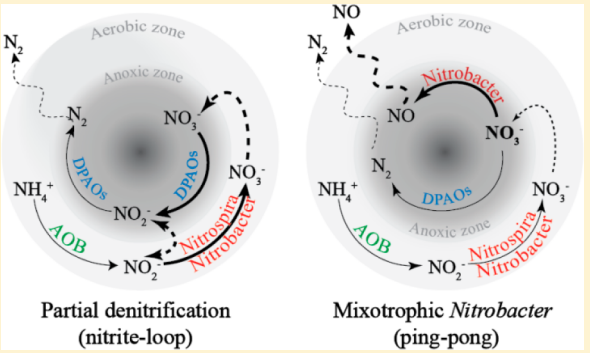

1. INTRODUCTION

From the first patent, to date, the application of aerobic granular sludge (AGS) for wastewater treatment has drawn a lot of attention to the fundamental process of granulation, the microbial population involved and the associated conversion processes.[1] This technology is based on self-immobilized granular-shaped biofilms operated in sequencing batch reactors (SBR) characterized by alternate anaerobic and aerobic phases and a short biomass settling time.[2]

Different redox layers (aerobic, anoxic, and anaerobic) within a single granule enable simultaneous carbon, nitrogen, and phosphate removal.[3] Functional bacterial groups in AGS are similar to the ones in conventional activated sludge (CAS), but significantly differ in general species composition.[4] This difference can partly be explained by the response of microorganisms to the feast−famine regimes, forcing them to accumulate storage polymers.[5] In acetate-fed AGS, an anaerobic feeding period is applied in which the acetate is converted to internal storage polymers (PHB) by polyphosphate accumulating organisms (PAOs) or glycogen accumulating organisms (GAOs). During the aerobic period, even though barely any organic carbon is left in the bulk liquid, PAOs and GAOs can still grow on their internally stored PHB and become the predominant heterotrophs in reactor.[3]

Unlike CAS, where *Nitrospira* is commonly found to be the dominant NOB with typical NOB/AOB ratios of 0.3−0.55,[6,7] *Nitrobacter* was reported to dominate the NOB population in AGS. Moreover, it was observed that in AGS the NOB/AOB ratios amounted to three, which is unusually high.[8,9] This elevated ratio implies that NOB grew uncoupled from the nitrite supplied by AOB.[9] While the *K*/*r* theory can be used to explain the predominance of *Nitrospira* in CAS,[10−12] in which continuous reactor operation favors the growth of K strategists (adapted to low substrate concentrations), two hypotheses were put forward[9] to explain the uncoupled growth of *Nitrobacter* from the nitrite produced by AOB in AGS. The first hypothesis suggested that a nitrite-loop occurred in the granular biofilm in which additional nitrite could become available from partial denitrification by heterotrophs. This is likely to occur because the reduction of NO_2^- to NO by nitrite reductases has been reported to be the rate limiting step in denitrification leading to nitrite accumulation in granule and even in the bulk liquid.[13] Besides, the involvement of different type of denitrifying PAOs (DPAOs) and denitrifying GAOs (DGAOs) with different pathways of denitrification[14−16] could lead to the availability of nitrite from denitrification in AGS.

The second hypothesis assumes a ping-pong effect in which mixotrophic *Nitrobacter* grow uncoupled from the nitrite supply of AOB. It is known that *Nitrobacter* is not an obligate autotroph and therefore not bound to energy generation from nitrite oxidation (lithoautotrophic growth) but can also grow

Received: April 17, 2015
Revised: August 3, 2015
Accepted: August 6, 2015
Published: August 6, 2015

DOI: 10.1021/acs.est.5b01952
Environ. Sci. Technol. 2015, 49, 11003−11010

heterotrophically on, e.g., acetate or pyruvate as electron donor and oxygen (aerobic growth) or nitrate as electron acceptors (dissimilatory nitrate reduction).[17−24] In all studies in which the growth on organic carbon was investigated, *Nitrobacter* showed the ability of storing and degrading internal storage polymers (PHB).[17,19,22] These metabolic activities have been confirmed by the genome sequence study on *Nitrobacter hamburgensis X14* and *Nitrobacter winogradskyi*.[25,26] Nitrite, ammonia, nitrous oxide (N_2O), and/or nitric oxide (NO) were reported to be produced during dissimilatory nitrate reduction.[22] However, the pathway by which N_2O would be formed is uncertain because the genome sequences (of the two NOB strains) were proven to lack nitric oxide reductase, meaning that denitrification would proceed until NO only.[25,26]

Mathematical modeling is a useful tool to gain insight in complex processes such as AGS[27−30] in which it is difficult to distinguish and identify the origin of specific conversion routes due to simultaneous biological conversions occurring in space and time. Therefore, in this study, mathematical models were set up to investigate the influence of partial denitrification and mixotrophic growth of NOB on the microbial distribution and community composition in AGS as well as potential NO generated from mixotrophic growth of *Nitrobacter*. Previously gathered experimental data[4,9] were used for model evaluation.

2. MATERIALS AND METHODS

2.1. Experimental Data. The mathematical model was based on the experimental setup as described by Winkler et al.[9] A lab-scale AGS reactor of 2.6 L was operated in cycles of 3 h, which were divided into four phases: 60 min anaerobic feeding; 112 min aeration period; 3 min settling, and 5 min effluent withdrawal. The dissolved oxygen concentration (DO) was controlled at 2 g O_2 m^{-3}, and pH was kept at 7. The volume exchange ratio was 57.7%. Per cycle, influent concentrations of 400 g COD m^{-3}, 50 g NH_4^+−N m^{-3}, and 20 g PO_4^{3-}−P m^{-3} were fed.

Microbial community distribution data were available over a period of 1 year from three different reactors:[9] two aerobic granular sludge reactors (lab- and pilot-scale) operated in SBR mode, and one activated sludge reactor. All samples were investigated with qPCR for their AOB/NOB ratios. qPCR was conducted as described earlier. Fluorescence in situ hybridization (FISH) was performed on granules in the same manner and with the same primers as recorded previously.[9]

2.2. Modeling Biological Conversion Processes. *2.2.1. Overview.* Several models describing simultaneous COD, nitrogen, and phosphate removal in aerobic granular sludge are available in literature.[29−34] In this study, the approach of de Kreuk et al.[29] was followed, including the growth of denitrifiers through the storage and degradation of internal polymers, which are important processes,[35] and only considering DPAOs and not DGAOs as denitrifying organisms. The competition between DPAOs and DGAOs has been extensively studied elsewhere[36] and is not addressed in the present study, which focuses on the nitrifier distribution in AGS.

A basic model was set up first, which served as a base case for the model extensions concerning the two individual hypotheses (nitrite-loop and ping-pong) and their combination (integrated model), as described below. In all models, four groups of bacteria were considered: DPAOs, AOB, and two NOB species, namely *Nitrospira* (NOB1) and *Nitrobacter* (NOB2). The stoichiometric matrices and kinetic expressions are summarized in SI Tables S1 and S2; stoichiometric and kinetic parameters are detailed in SI Tables S3 and S4, respectively. Reactor and granule characteristics, operating conditions, and mass transfer parameters are listed in SI Table S5.

2.2.2. Basic Model. In the basic model, the denitrification processes of DPAOs were defined as single-step denitrification, converting nitrate directly to nitrogen gas (Figure 1A). Under

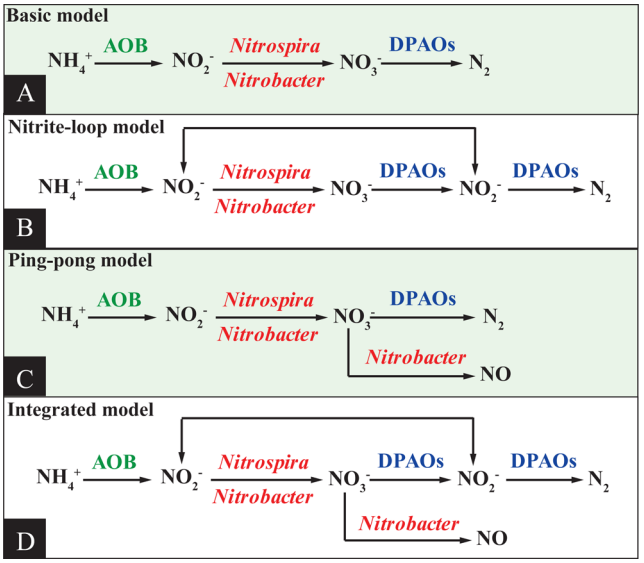

Figure 1. Overview of nitrogen conversion pathways and involved bacterial groups modeled in this study. All models included NH_4^+ oxidation (nitritation) by AOB followed by NO_2^- oxidation (nitratation) by *Nitrospira* and *Nitrobacter* and were further characterized by (A) single-step denitrification performed by DPAOs; (B) two-step denitrification by DPAOs (NO_2^- available for both denitrification and nitratation); (C) single-step denitrification by DPAOs and dissimilatory nitrate reduction by *Nitrobacter*; (D) two-step denitrification by DPAOs (NO_2^- available for both denitrification and nitratation) and dissimilatory nitrate reduction by *Nitrobacter*.

anaerobic conditions, DPAOs convert acetate to PHB by using energy gained from oxidizing glycogen and releasing poly phosphate (poly-P) (process 1, SI Table S1). Anaerobic maintenance on poly-P takes place as well (process 2). Under aerobic or anoxic conditions, by using oxygen or NOx, respectively, DPAOs grow on PHB (processes 3 and 7.I), restore the glycogen (processes 4 and 8.I) and poly-P pools (processes 5 and 9.I), and carry out maintenance (processes 6 and 10.I). The decay process of DPAOs (process 15) was introduced to maintain the structure of granule.[29] The biological conversion processes of nitrifiers followed existing models, e.g., of Volcke et al.[37] In the aeration period, ammonia is converted via nitrite into nitrate by AOB and NOB (processes 16, 20, and 24). Endogenous respiration for autotrophic organisms was included and leads to the production of inert material (processes 17−19, 21−23, and 25−27).

2.2.3. Nitrite-Loop Model. The nitrite-loop model was based on two-step denitrification to evaluate the influence of the availability of intermediate NO_2^- for uptake by NOB (Figure 1B). The denitrification pathway of DPAOs was defined to occur via nitrate with nitrite as intermediate (NO_3^- → NO_2^- → N_2). This was implemented by replacing the processes 7I, 8I, 9I, and 10I (NO_3^- → N_2) of the basic model by the processes

DOI: 10.1021/acs.est.5b01952
Environ. Sci. Technol. 2015, 49, 11003−11010

Table 1. Model Calibration in Terms of Substrate Profile and Nitrifier Biomass

model	features	performance in describing experimental data[a]		
		substrate profile	NOB/AOB ratio (2−5)	*Nitrospira* and *Nitrobacter*
basic	single-step denitrification	+	−	− (coexistence)
nitrite-loop	two-step denitrification	+	+	− (coexistence)
ping-pong	single-step denitrification and mixotrophic *Nitrobacter*	+	−	+ (*Nitrobacter* completely dominates)
integrated	two-step denitrification and mixotrophic *Nitrobacter*	+	+	+ (*Nitrobacter* completely dominates)

[a]+ Model described experimental data well; − Model could not describe experimental data.

7II, 8I, 9II, and 10II ($NO_3^- \rightarrow NO_2^-$) and 11, 12, 13, and 14 ($NO_2^- \rightarrow N_2$) (SI Table S1).

2.2.4. Ping-Pong Model. The ping-pong model was based on the basic model, which was extended with the capability of *Nitrobacter* to grow mixotrophically (Figure 1C). In the anaerobic feeding phase, NO_3^- remaining from the previous cycle could be used by *Nitrobacter* as an electron acceptor to take up acetate and store it as PHB (process 28: acetate + $NO_3^- \rightarrow NH_4$ + PHB) as it was suggested to occur in batch tests.[22] In the aeration phase, PHB was assumed to be oxidized with either O_2 as electron acceptor (process 29: PHB + $O_2 \rightarrow$ NOB2 biomass) or NO_3^- as electron acceptor (process 30: PHB + $NO_3^- \rightarrow$ NO + NOB2 biomass).[17,19] Although some cultures of *Nitrobacter* were reported to release N_2O through dissimilatory nitrate reduction,[22] two strains were identified lacking the nitric oxide reductase (to reduce NO to N_2O).[25,26] For this reason, NO was chosen as the end product as described by reaction 30, SI Table S1).

Nitric oxide (S_{NO}) and PHB (X_{PHB}^{NOB2}) were included as two additional state variables to describe dissimilatory nitrate reduction and internal PHB storage for *Nitrobacter*. The kinetic expressions of *Nitrobacter* describing the capability of producing and consuming PHB were adapted from those for DPAOs (SI Table 2, processes 28, 29, and 30). This involved the definition of additional parameters for *Nitrobacter*, namely, the maximum acetate uptake rate ($q_{Ac,AN}^{NOB2}$), maximum aerobic PHB degradation rate ($q_{PHB,OX}^{NOB2}$), maximum storage capacity of PHB ($f_{PHB,max}^{NOB2}$), and affinity constant to nitrate, PHB, and acetate (K_{NO3}^{NOB2}, K_{PHB}^{NOB2} and K_{Ac}^{NOB2}, respectively). The stoichiometric yields of *Nitrobacter* in the above reactions (Y_{PHB}^{NOB2}, $Y_{PHB,OX}^{NOB2}$ and $Y_{PHB,NO3}^{NOB2}$) were obtained from parameter estimation, using the corresponding values for DPAOs as initial values (SI Table S6).

2.2.5. Integrated Model. An integrated model was established combining the ping-pong and nitrite-loop pathways (Figure 1D) to assess the combined influence of the nitrite-loop and ping-pong hypotheses on the nitrifier distribution.

2.3. Reactor and Simulation Setup. A 1-dimensional biofilm model (considering radial gradients only) including the above-mentioned conversion processes was developed and implemented in AQUASIM,[38] which has previously proven its suitability for describing biological processes occurring in granular sludge reactors.[29,32,39] Simulating the SBR fill and discharge processes was done according to Beun et al.[27] The steady state diameter of granule (r_{max}) was set at typical value of 1.2 mm. The porosity of granule was considered constant and homogeneous throughout the granule. To maintain r_{max}, a detachment (u_{Det}) was introduced when growth velocity of granule was positive.[37] The number of granules was calculated from the volume of sludge in the reactor (0.9 L). The density of bacteria and storage compound was set at 350,000 kg m^{-3}. Other parameters and setups regarding the reactor and granule characteristic are detailed in SI Table S5.

The reference operating conditions involved a temperature of 20 °C and a dissolved oxygen concentration of 2 g O_2 m^{-3}. Each model was simulated until steady state was reached in the sense that effluent concentrations (at the end of each cycle) and active biomass concentrations did not change more than 1%, which was mostly the case after 500−800 days (SI Figure S1).[29] This time period was judged reasonable, given that in laboratory experiments, stable operation in terms of bulk liquid concentrations is typically achieved between 4 and 12 months, while getting stable biomass concentration profiles may take longer,[40] depends on the initial conditions. To assess the influence of operational conditions, the parameters of interest were varied while all others were kept constant at reference simulation conditions. The varied parameters were granule radius (0.4 to 0.9 mm), temperature (10 to 30 °C), and DO (0.5 to 6 g O_2 m^{-3}).

2.4. Model Calibration. Model calibration was performed by trial and error through extensive simulations by adjusting parameter values of concern (SI Table S6). Results from each simulation were compared with experimental data. The required accuracy between simulated data and experimental data after calibration was set at 10% considering the uncertainty associated with other parameters (e.g., exact granule size distribution and granule surface area).[29] For instance, the active biomass fraction (ε_T) was estimated to obtain a biomass concentration of 20 kg VSS m^{-3}, as experimentally measured (SI Table S8). The bioconversion rates of NH_4^+, PO_4^{3-}, and NO_3^- at steady state were compared to experimental data by adjusting the parameters of DPAOs ($q_{PP,OX}^{PAO}$ and Y_{PO4}^{PAO}) and the parameter of AOB (μ_{max}^{AOB}, which was known to have high influence on ammonium and nitrate profiles).[29] The simulated nitrifier distribution (ratio of NOB to AOB and of *Nitrobacter* to *Nitrospira*) was fitted to the qPCR results by adjusting the NOB2 parameters (Y_{PHB}^{NOB2}, $Y_{PHB,OX}^{NOB2}$, and $Y_{PHB,NO3}^{NOB2}$), which are unique for the ping-pong and integrated models presented in this study. It is important to note that the kinetic parameters of *Nitrospira* and *Nitrobacter* (μ_{max}^{NOB1}, μ_{max}^{NOB2}, K_{O2}^{NOB1}, K_{O2}^{NOB2}, K_{NO2}^{NOB1}, and K_{NO2}^{NOB2}) and their growth yield on nitrite (Y_{NOB1} and Y_{NOB2} were kept constant as their values were taken from literature and followed all conditions being important to their *K/r* strategy.[6,10,11,41,42] A similar net growth rate of DPAOs for the single-step denitrification (basic) model and for the two-step denitrification (nitrite-loop) model was achieved by adjusting the reduction factor (η_{NOx}^{PAO}) and anoxic maintenance (m_{AX}^{PAO}) values of DPAOs under anoxic conditions, given that literature values for single-step denitrification were available. This is necessary because the two-step denitrification involves $2e^-$ for nitrate reduction and $3e^-$ for nitrite reduction, while $5e^-$ are used during single-step denitrification from NO_3^- to N_2.[33,43]

DOI: 10.1021/acs.est.5b01952
Environ. Sci. Technol. 2015, 49, 11003−11010

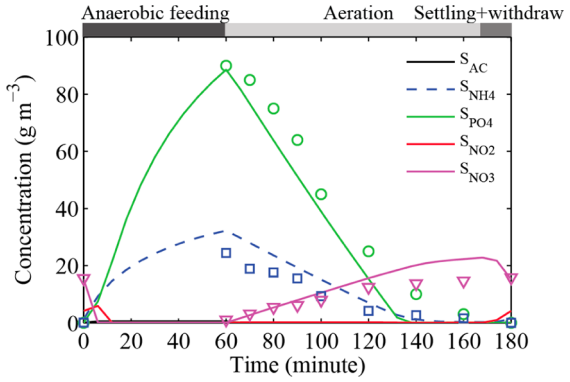

Figure 2. Steady state substrate profile of a typical operational cycle for integrated model with granule radius = 0.6 mm, DO = 2 g O_2 m^{-3}, and temperature = 20 °C. Lines indicate simulated substrate concentration and markers indicate the measured concentration[9] of phosphate (○), ammonium (□), and nitrate (▽). Data of acetate (S_{AC}) and nitrite (S_{NO2}) are not shown since they are quickly consumed resulting in a very low bulk concentration.

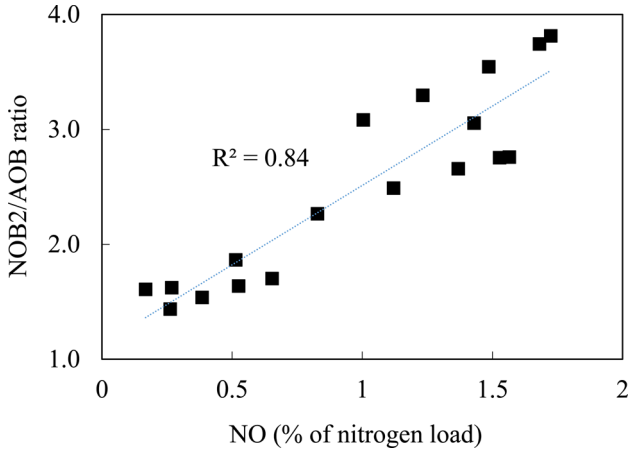

Figure 4. Relation between NO and *Nitrobacter*/AOB ratio in AGS. Simulation results for integrated model with various operational conditions (granule size = 0.4 to 0.9 mm, temperature = 10 to 30 °C, and DO = 0.5 to 6 g O_2 m^{-3}).

3. RESULTS AND DISCUSSION

3.1. Model Evaluation with Experimental Data. All models were able to describe the substrate profile of the lab-scale AGS. Nevertheless, only the integrated model corresponded with the experimental data in terms of elevated NOB/AOB ratio and dominance of *Nitrobacter* (Table 1). This best fit was consistent with the considered parameter range (SI Table S6). Therefore, the calibrated parameter values for integrated model were applied for all model setups.

The substrate profiles during cyclic operation (Figure 2) and the bioconversion rates (SI Table S7) simulated with the integrated model fitted the experimental data very well. During the anaerobic feeding phase, the acetate concentration was almost zero due to fast consumption for PHB storage by DPAOs, while phosphate was released.[44] The fed ammonium

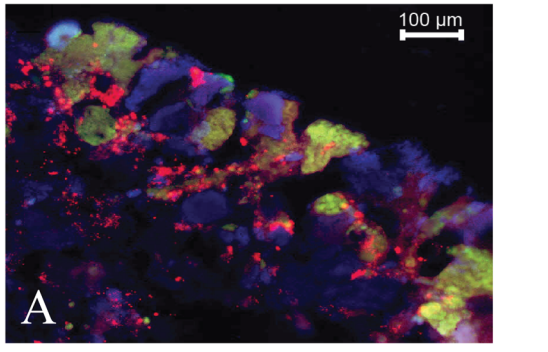

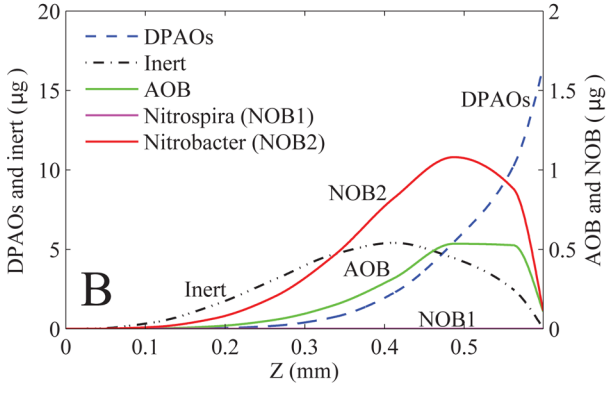

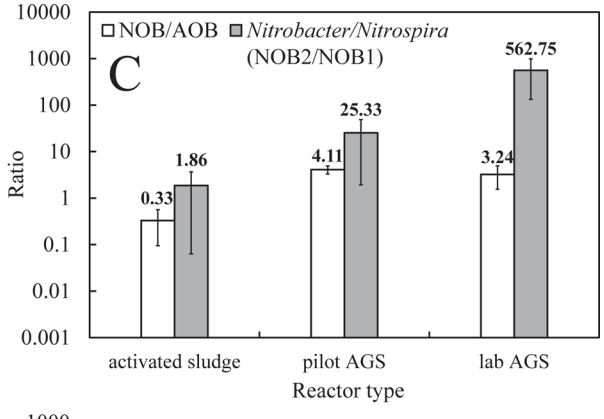

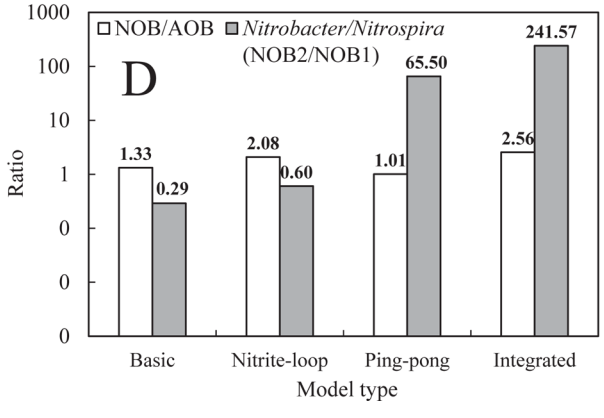

Figure 3. Bacterial distribution in granule. (A) FISH image of sliced granule: AOB (green), NOB (red), DPAOs (blue).[9] (B) Simulated biomass profile of granule obtained with the integrated model (for granule radius = 0.6 mm, DO = 2 g O_2 m^{-3}, temperature = 20 °C), *Z* = distance in mm from granule core. (C) Experimentally determined NOB/AOB and *Nitrobacter*/*Nitrospira* ratios for several reactor types.[9] (D) Simulated NOB/AOB and *Nitrobacter*/*Nitrospira* ratios with four model setups (for granule radius = 0.6 mm, DO = 2 g O_2 m^{-3}, temperature = 20 °C).

DOI: 10.1021/acs.est.5b01952
Environ. Sci. Technol. 2015, 49, 11003−11010

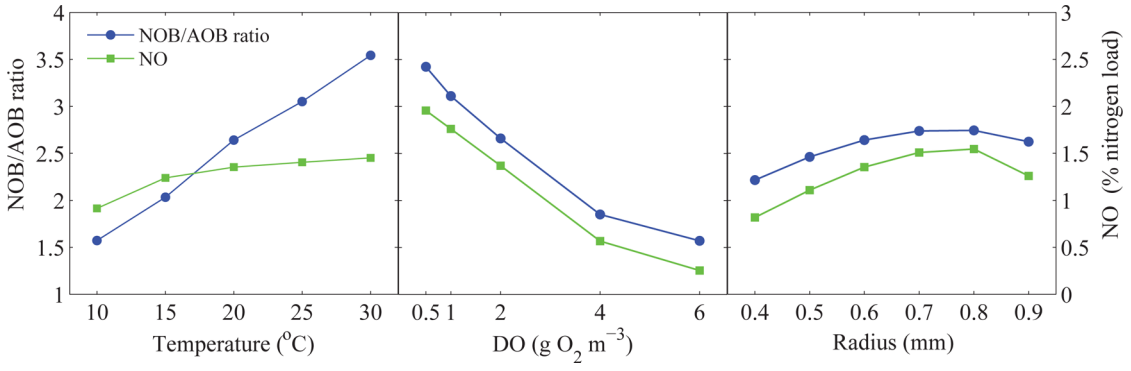

Figure 5. Influence of operational conditions on biomass distribution of nitrifiers and potential NO emission.

was not converted, causing an increase in its concentration during this phase. Given that the reactor is not mixed, representative liquid sampling is not possible during anaerobic feeding (no experimental data available). In the aeration phase, ammonium was converted to nitrate by nitrifiers in the aerobic layer of the granules (oxygen penetration depth is defined by diffusion, oxygen concentration in the bulk, and by oxygen consumption of organisms). Simultaneously, phosphate was used by DPAOs for poly-P formation while consuming stored PHB either with oxygen in aerobic layers or with nitrite or nitrate as electron acceptor in the anoxic layers of the granule. The simulated removal efficiency of COD, phosphate, and nitrogen were 100%, 100%, and 60%, respectively, which were also comparable to the experimental data.

The model successfully described the total biomass concentration in reactor of 20 ± 2 kg m^{-3}. The simulated total biomass of AOB, DPAOs, and inert material for four models was essentially the same, as reflected by a small standard deviation (1.42 ± 0.06, 19.2 ± 0.32, and 15.92 ± 0.22 g of VSS per 2.6 L reactor, respectively, detailed in SI Table S8). As expected, the simulated amount of NOB biomass significantly differed between the four models under study. The basic and nitrite-loop model predicted that *Nitrospira* and *Nitrobacter* coexist in granules but that *Nitrospira* was present in higher amounts (NOB2/NOB1 = 0.29 and 0.6), while the ping-pong and the integrated model simulated the dominance of *Nitrobacter* over *Nitrospira* (NOB2/NOB1 ≫ 1) (Figure 3D).

3.2. Influence of Partial Denitrification. The nitrifier distribution was compared between the basic model (single-step denitrification) and the nitrite-loop model (two-step denitrification) to examine the influence of additional nitrite supply from partial denitrification (nitrite-loop). For both models, *Nitrobacter* and *Nitrospira* could coexist in one granule, but *Nitrospira* was dominant (*Nitrobacter*/*Nitrospira* ratio of 0.29 and 0.6, Figure 3D). The simulated amount of NOB biomass was 30% higher than that of AOB for the basic model and even 100% higher for the nitrite-loop model (NOB/AOB ratio of 1.33 and 2.08, respectively, Figure 3D). The 60% increase in the amount of NOB for the nitrite-loop model compared to the basic model was attributed to a doubling in the biomass concentration of *Nitrobacter* and a 20% increase in that of *Nitrospira*.

The availability of nitrite in aerobic granules was observed experimentally, and it was shown that the reduction of nitrate to nitrite was mainly mediated by DGAOs,[45] whereas the produced nitrite was then further denitrified to dinitrogen gas by DPAOs (clade II) and to the lesser extent by DPAOs (clade I), without being oxidized to nitrate by NOB.[46] However, a particular type of DPAOs (clade II) can only use nitrite (and not nitrate) as electron acceptor and can hence remove excess nitrite from the bulk potentially suppressing the nitrite-loop (reoxidation of nitrite by NOB). Since it is known that high temperatures (>20 °C) and low pH (<7) favor the growth of DGAOs over DPAOs,[35,36,47] it can be assumed that the availability of nitrite in the granule will be higher under these conditions, promoting the nitrite-loop as it was also shown in the simulations here. From an engineering perspective, an accelerated nitrite-loop is unfavorable because it lowers the nitrogen removal efficiency. Efficient control strategies toward a DPAOs dominated culture at high temperature are possible due to selective removal of smaller granules, which have been shown to be dominated by GAOs.[48]

A number of studies reported that *Nitrospira* is present in nitrifying systems in equal or even higher numbers compared to AOB.[49−51] Because AOB oxidize the same quantity of nitrogen as NOB, the yield is the main differentiating factor in the relative population size of the two types of nitrifying organisms.[42] Within the NOB population, the coexistence of *Nitrobacter* and *Nitrospira* can be explained by niche separation in space created by substrate concentration gradients in the granule and/or in time created by continuous alternating regime of SBR.[41,49] For the basic model (no mixotrophic growth of NOB) the nitrite affinity rather than the oxygen affinity (K_O) and/or the maximum growth rate was the factor determining the NOB distribution. The half saturation constant of nitrite for *Nitrospira* (K_{NO2}^{NOB1} = 0.27 g NO_2−N m^{-3}) is significantly lower than the one of *Nitrobacter* (K_{NO2}^{NOB2} = 0.39 g NO_2−N m^{-3}), while the maximum growth rate and K_O values are in favor of *Nitrobacter* (K_{O2}^{NOB1} = 0.54 g O_2 m^{-3}, μ_{max}^{NOB1}= 0.37 d^{-1} and K_{O2}^{NOB2} = 0.43 g O_2 m^{-3}, μ_{max}^{NOB2} = 0.495 d^{-1}).[36] For the basic model, the simulated nitrite concentrations in the bulk as well as in granule were very low (0.1−0.3 mg NO_2−N L^{-1}) during the aeration phase (SI Figure S2A,B), which favored *Nitrospira* and led to their dominance. For the nitrite-loop model, the simulated nitrite concentration in the granule during the aeration phase was 40% higher than that of the basic model, resulting in an increased proportion of *Nitrobacter* biomass (*Nitrobacter*/*Nitrospira* ratio 0.60 for nitrite-loop model versus 0.29 for the basic model) because they are better competitors in environments with high nitrite concentrations (*r*-strategist).[12]

Overall, even though the nitrifier distributions simulated with the basic and nitrite-loop model failed to explain observations from the granular pilot and lab-scale reactor in terms of dominance of *Nitrobacter*, the partial denitrification taken up in the nitrite-loop model did result in an elevated NOB/AOB ratio. Part of the nitrite produced by DPAOs was quickly

DOI: 10.1021/acs.est.5b01952
Environ. Sci. Technol. 2015, 49, 11003−11010

oxidized to nitrate by NOB in the oxygen penetrated zone of the granule. Part of this nitrate produced by NOB was then denitrified again by DPAOs to generate more nitrite (due to partial denitrification), which then was looped back to NOB eventually uncoupling the growth of NOB from nitrite produced by AOB (Figure 3C,D).

3.3. Influence of NOB Mixotrophic Growth. The basic model and ping-pong model were compared to study the influence of the mixotrophic growth of *Nitrobacter*. A similar NOB/AOB ratio (1.01 versus 1.33) but a significantly higher *Nitrobacter*/*Nitrospira* ratio (65 versus 0.29) was found for the ping-pong model than for the basic model (Figure 3D). The capability of *Nitrobacter* to grow mixotrophically led to its complete dominance, which fitted the experimental data well (Figure 3C,D). However, the NOB/AOB ratio was not elevated and even lower than that for basic model. This lower ratio can be explained by the fact that *Nitrobacter* has a lower autotrophic yield (0.072 g COD g^{-1} N) compared to the autotrophic yield of *Nitrospira* (0.11 g COD g^{-1} N). Therefore, the NOB/AOB ratio will be lower in a system dominated by autotrophic *Nitrobacter* compared to a reactor receiving the same amount of nitrite but dominated by *Nitrospira*.

The possible production of PHB by various type of bacteria is a fact.[52] Especially feast−famine regimes, as present in an aerobic granular sludge reactor, will trigger the growth of organisms with the ability to produce PHA.[53] In the simulated experiments *Nitrobacter* was periodically subjected to nitrate (15 mg L^{-1} remain from previous cycle) and acetate (in feeding solution), which stimulated it to store PHB.[16,21] The simulated amount of acetate assimilated by *Nitrobacter* was low (7.2 mg of COD acetate per cycle) because they had to compete with DPAOs for acetate. Nevertheless, heterotrophic growth of *Nitrobacter* still contributed to 30% of the total biomass of *Nitrobacter*. In addition, the maximum heterotrophic growth rate of *Nitrobacter* for the models was 4−8 times faster (depend on electron acceptor) compared to its maximum autotrophic growth rate, which was in agreement with earlier report,[24] hence creating a selective advantage for *Nitrobacter*. It is important to note that *Nitrobacter* was proven to be the predominant NOB (*Nitrobacter*/*Nitrospira* ratio of 3) in a reactor subjected to alternate substrate availability, confirming that SBR operation selects for *Nitrobacter*.[6]

Overall, despite that the integration of dissimilatory nitrate reduction in the ping-pong model led to the experimentally observed dominance of *Nitrobacter*, the model could not explain the experimentally observed elevation in NOB/AOB ratio (Figure 3C,D).

3.4. Combined Effect. The stand-alone nitrite-loop and ping-pong models could only partly explain experimental observations. The nitrite-loop model led to elevated NOB/AOB ratio, while the ping-pong model explained the dominance of *Nitrobacter* (and not *Nitrospira*). By combining both pathways in the integrated model, a NOB/AOB ratio of 2.56 was simulated, which fitted the experimentally observed NOB distribution for AGS well (Figure 3D). Heterotrophic growth of *Nitrobacter* contributed to 38% of their total biomass (2.22 g of heterotrophic growth from 6.77 g of COD acetate consumed compare to 3.58 g of autotrophic growth per cycle) and led to their complete dominance over *Nitrospira* (*Nitrobacter*/*Nitrospira* ratio of 241.57). Compared to the ping-pong model, the extra nitrite available from partial denitrification in the integrated model facilitated the autotrophic growth of NOB and hence further increase the NOB/AOB ratio as well as NOB2/NOB1 ratio (synergistic effect of autotrophic and heterotrophic growth of *Nitrobacter*). The spatial distribution of the autotrophs (AOB and NOB) and heterotrophs (DPAOs) simulated with the integrated model was in accordance with the FISH analysis results (Figure 3A,B). The nitrifiers were mainly located in the outer layer, while the DPAOs were presented throughout the granule. Mixotrophic *Nitrobacter* were able to grow in deeper anoxic layers because of their mixotrophic growth (Figure 3A,B). The results presented in this study clearly demonstrate that the biomass distribution of nitrifiers in the AGS reactor was the result of both the availability of nitrite in granule and the mixotrophic growth of Nitrobacter. Only the combination of both pathways led to an elevated NOB/AOB ratio and to the dominance of *Nitrobacter*.

3.5. Potential End Products of Mixotrophic Growth of *Nitrobacter*. In this study, NO was considered to be the end product of mixotrophic NOB activity. The simulated amount of released NO amounted to 0.69 g NO−N m^{-3} (1.37% of the nitrogen load) per cycle. There was a significant positive correlation between the NOB2/AOB ratio and the NO released (R^2 = 0.84, Figure 4) reflecting a higher NO emission from AGS as the mixotrophic growth of *Nitrobacter* is promoted. As for the end product, previous studies have shown controversial results that ammonia, nitrite, and N_2O were emitted from mixotrophically grown *Nitrobacter* cultures,[22] whereas genome studies of two *Nitrobacter* strains proved the lack of NOR genes,[25] indicating that only NO could be the end product of *Nitrobacter* dissimilatory nitrate reduction. Since the genomes of other strains are not known, it cannot be excluded that they play a role in the formation of other products. However, the complexity of microbial interactions in the granules makes it difficult to draw clear conclusions on which organism or metabolic pathways can possibly contribute to N_2O emission.

3.6. Influence of Operating Conditions on Biomass Distribution and NO emission. The simulated influence of temperature, DO, and granule size (radius) on NO emission and NOB/AOB ratio is summarized in Figure 5. More extensive simulation results varying these parameters simultaneously and analyzing the statistical significance are summarized in SI Table S10.

The NOB/AOB ratio increased from 1 to 3.8 with an increase in temperature from 10 to 30 °C (Figure 5A). Since the endogenous respiration rate of AOB (b_{AOB}) is higher and increases faster than that of *Nitrobacter*[54] (b_{NOB2}) with increasing temperature, higher temperatures will lead to a higher NOB/AOB ratio. In addition, the degradation rate of PHB by *Nitrobacter* will be higher at higher temperatures, which explains higher NO released associated with mixotrophic growth at higher temperature (Figure 5).

As the bulk oxygen concentration decreased, oxygen penetration in the granule became the limiting factor on the rate of biological conversion processes resulting in a higher anoxic volume fraction available for mixotrophic growth and thus higher NO released at lower DO (Figure 5).

A changing granule size, within a range that is reasonably to be expected, only has a limited effect on the NOB/AOB ratio and NO emission. From radius of 0.4 to 0.7 mm, the increased NO emission can be attributed to the increased anoxic volume fraction, which facilitated the NO production (process 30, SI Table S1). Nevertheless, beyond a certain granule size (between 0.7 and 0.8 mm), the NOB/AOB ratio and the NO emission decreased with increasing granule size. This can be attributed to limitations of surface area for oxygen transport,

DOI: 10.1021/acs.est.5b01952
Environ. Sci. Technol. 2015, 49, 11003−11010

resulting in a smaller aerobic volume fraction in larger granules. Combined with the fact that the oxygen affinity constant of NOB is lower than that of AOB ($K_{O2}^{AOB} > K_{O2}^{NOB}$), the biomass of NOB will be lowered at lower oxygen concentrations, which accordingly led to a decrease in NOB biomass and hence in lower NO production.

Overall, an increasing temperature or decreasing DO resulted in increase of the NOB/AOB ratio and of the NO emissions, while a change in granule size had minor influence.

■ ASSOCIATED CONTENT

Supporting Information

The Supporting Information is available free of charge on the ACS Publications website at DOI: 10.1021/acs.est.5b01952.

Model setup and additional results with 24 pages containing 10 tables (Table S1 to S10) and two figures (Figure S1 and S2) (PDF)

■ AUTHOR INFORMATION

Corresponding Author

*E-mail: Eveline.Volcke@UGent.be.

Author Contributions

§These authors contributed equally to this work. The manuscript was written through contributions of all authors. All authors have given approval to the final version of the manuscript.

Notes

The authors declare no competing financial interest.

■ ACKNOWLEDGMENTS

M.-K.H.W. was funded by a Marie Curie Intra-European fellowship (PIEF-GA-2012-329328).

■ ABBREVIATIONS

AGS	aerobic granular sludge
AOB	ammonia oxidizing bacteria
ASM	activated sludge model
BOD	biological oxygen demand
COD	chemical oxygen demand
DPAOs	denitrifying polyphosphate accumulating organisms
DGAOs	denitrifying glycogen accumulating organisms
EBPR	enhanced biological phosphate removal
GAOs	glycogen accumulating organisms
NOB	nitrite oxidizing bacteria
PAOs	polyphosphate accumulating organisms
PHB	poly beta-hydroxyl butyrate
poly-P	polyphosphate
SBR	sequencing batch reactor
WWTP	wastewater treatment plant

■ REFERENCES

(1) Adav, S. S.; Lee, D. J.; Show, K. Y.; Tay, J. H. Aerobic granular sludge: recent advances. *Biotechnol. Adv.* **2008**, *26* (5), 411−23.

(2) Liu, Y.; Wang, Z. W.; Qin, L.; Liu, Y. Q.; Tay, J. H. Selection pressure-driven aerobic granulation in a sequencing batch reactor. *Appl. Microbiol. Biotechnol.* **2005**, *67* (1), 26−32.

(3) de Kreuk, M.; Heijnen, J. J.; van Loosdrecht, M. C. M. Simultaneous COD, nitrogen, and phosphate removal by aerobic granular sludge. *Biotechnol. Bioeng.* **2005**, *90* (6), 761−769.

(4) Winkler, M. K.; Kleerebezem, R.; de Bruin, L. M.; Verheijen, P. J.; Abbas, B.; Habermacher, J.; van Loosdrecht, M. C. Microbial diversity differences within aerobic granular sludge and activated sludge flocs. *Appl. Microbiol. Biotechnol.* **2013**, *97* (16), 7447−58.

(5) Beun, J. J.; Dircks, K.; van Loosdrecht, M. C. M.; Heijnen, J. J. Poly-beta-hydroxybutyrate metabolism in dynamically fed mixed microbial cultures. *Water Res.* **2002**, *36* (5), 1167−1180.

(6) Dytczak, M. A.; Londry, K. L.; Oleszkiewicz, J. A. Activated sludge operational regime has significant impact on the type of nitrifying community and its nitrification rates. *Water Res.* **2008**, *42* (8−9), 2320−2328.

(7) You, S. J.; Chuang, S. H.; Ouyang, C. F. Nitrification efficiency and nitrifying bacteria abundance in combined AS-RBC and A2O systems. *Water Res.* **2003**, *37* (10), 2281−2290.

(8) Carvalho, G.; Meyer, R. L.; Yuan, Z. G.; Keller, J. Differential distribution of ammonia- and nitrite-oxidising bacteria in flocs and granules from a nitrifying/denitrifying sequencing batch reactor. *Enzyme Microb. Technol.* **2006**, *39* (7), 1392−1398.

(9) Winkler, M. K.; Bassin, J. P.; Kleerebezem, R.; Sorokin, D. Y.; van Loosdrecht, M. C. Unravelling the reasons for disproportion in the ratio of AOB and NOB in aerobic granular sludge. *Appl. Microbiol. Biotechnol.* **2012**, *94* (6), 1657−66.

(10) Kim, D. J.; Kim, S. H. Effect of nitrite concentration on the distribution and competition of nitrite-oxidizing bacteria in nitratation reactor systems and their kinetic characteristics. *Water Res.* **2006**, *40* (5), 887−894.

(11) Nogueira, R.; Melo, L. F. Competition between Nitrospira spp. and Nitrobacter spp. in nitrite-oxidizing bioreactors. *Biotechnol. Bioeng.* **2006**, *95* (1), 169−175.

(12) Schramm, A.; de Beer, D.; van den Heuvel, J. C.; Ottengraf, S.; Amann, R. Microscale distribution of populations and activities of Nitrosospira and Nitrospira spp. along a macroscale gradient in a nitrifying bioreactor: Quantification by in situ hybridization and the use of microsensors. *Appl. Environ. Microbiol.* **1999**, *65* (8), 3690−3696.

(13) Firestone, M. K.; Firestone, R. B.; Tiedje, J. M. Nitric-Oxide as an Intermediate in Denitrification - Evidence from N-13 Isotope Exchange. *Biochem. Biophys. Res. Commun.* **1979**, *91* (1), 10−16.

(14) Zeng, R. J.; Yuan, Z. G.; Keller, J. Enrichment of denitrifying glycogen-accumulating organisms in anaerobic/anoxic activated sludge system. *Biotechnol. Bioeng.* **2003**, *81* (4), 397−404.

(15) Carvalho, G.; Lemos, P. C.; Oehmen, A.; Reis, M. A. M. Denitrifying phosphorus removal: Linking the process performance with the microbial community structure. *Water Res.* **2007**, *41* (19), 4383−4396.

(16) Wang, X. L.; Zeng, R. J.; Dai, Y.; Peng, Y. Z.; Yuan, Z. G. The denitrification capability of cluster 1 Defluviioccus vanus-related glycogen-accumulating organisms. *Biotechnol. Bioeng.* **2008**, *99* (6), 1329−1336.

(17) Smith, A. J.; Hoare, D. S. Acetate Assimilation by Nitrobacter Agilis in Relation to Its Obligate Autotrophy. *J. Bacteriol.* **1968**, *95* (3), 844.

(18) Faull, K. F.; Wallace, W.; Nicholas, D. J. Nitrite Oxidase and Nitrate Reductase in Nitrobacter Agilis. *Biochem. J.* **1969**, *113* (3), 449.

(19) Van Gool, A. P.; Tobback, P. P.; Fischer, I. Autotrophic Growth and Synthesis of Reserve Polymers in Nitrobacter-Winogradskyi. *Arch. Microbiol.* **1971**, *76* (3), 252.

(20) Steinmuller, W.; Bock, E. Growth of Nitrobacter in the presence of organic matter. I. Mixotrophic growth. *Arch. Microbiol.* **1976**, *108* (3), 299−304.

(21) Steinmuller, W.; Bock, E. Enzymatic Studies on Autotrophically, Mixotrophically and Heterotrophically Grown Nitrobacter-Agilis with Special Reference to Nitrite Oxidase. *Arch. Microbiol.* **1977**, *115* (1), 51−54.

(22) Freitag, A.; Rudert, M.; Bock, E. Growth of Nitrobacter by Dissimilatoric Nitrate Reduction. *FEMS Microbiol. Lett.* **1987**, *48* (1−2), 105−109.

(23) Bock, E.; Wilderer, P. A.; Freitag, A. Growth of Nitrobacter in the Absence of Dissolved-Oxygen. *Water Res.* **1988**, *22* (2), 245−250.

DOI: 10.1021/acs.est.5b01952
Environ. Sci. Technol. 2015, 49, 11003−11010

(24) Bock, E.; Koops, H. P.; Moller, U. C.; Rudert, M. A New Facultatively Nitrite Oxidizing Bacterium, Nitrobacter-Vulgaris Sp-Nov. *Arch. Microbiol.* **1990**, *153* (2), 105−110.
(25) Starkenburg, S. R.; Chain, P. S. G.; Sayavedra-Soto, L. A.; Hauser, L.; Land, M. L.; Larimer, F. W.; Malfatti, S. A.; Klotz, M. G.; Bottomley, P. J.; Arp, D. J.; Hickey, W. J. Genome sequence of the chemolithoautotrophic nitrite-oxidizing bacterium Nitrobacter winogradskyi Nb-255. *Appl. Environ. Microbiol.* **2006**, *72* (3), 2050−2063.
(26) Starkenburg, S. R.; Larimer, F. W.; Stein, L. Y.; Klotz, M. G.; Chain, P. S. G.; Sayavedra-Soto, L. A.; Poret-Peterson, A. T.; Gentry, M. E.; Arp, D. J.; Ward, B.; Bottomley, P. J. Complete genome sequence of Nitrobacter hamburgensis X14 and comparative genomic analysis of species within the genus Nitrobactei. *Appl. Environ. Microbiol.* **2008**, *74* (9), 2852−2863.
(27) Beun, J. J.; Heijnen, J. J.; van Loosdrecht, M. C. M. N-removal in a granular sludge sequencing batch airlift reactor. *Biotechnol. Bioeng.* **2001**, *75* (1), 82−92.
(28) Su, K. Z.; Yu, H. Q. A generalized model for aerobic granule-based sequencing batch reactor. 1. Model development. *Environ. Sci. Technol.* **2006**, *40* (15), 4703−4708.
(29) de Kreuk, M. K.; Picioreanu, C.; Hosseini, M.; Xavier, J. B.; van Loosdrecht, M. C. Kinetic model of a granular sludge SBR: influences on nutrient removal. *Biotechnol. Bioeng.* **2007**, *97* (4), 801−15.
(30) Xavier, J. B.; De Kreuk, M. K.; Picioreanu, C.; van Loosdrecht, M. C. M. Multi-scale individual-based model of microbial and bioconversion dynamics in aerobic granular sludge. *Environ. Sci. Technol.* **2007**, *41* (18), 6410−6417.
(31) Ni, B. J.; Yu, H. Q.; Sun, Y. J. Modeling simultaneous autotrophic and heterotrophic growth in aerobic granules. *Water Res.* **2008**, *42* (6−7), 1583−1594.
(32) Vazquez-Padin, J. R.; Mosquera-Corral, A.; Campos, J. L.; Mendez, R.; Carrera, J.; Perez, J. Modelling aerobic granular SBR at variable COD/N ratios including accurate description of total solids concentration. *Biochem. Eng. J.* **2010**, *49* (2), 173−184.
(33) Zhou, M.; Gong, J. Y.; Yang, C. Z.; Pu, W. H. Simulation of the performance of aerobic granular sludge SBR using modified ASM3 model. *Bioresour. Technol.* **2013**, *127*, 473−481.
(34) Kagawa, Y.; Tahata, J.; Kishida, N.; Matsumoto, S.; Picioreanu, C.; van Loosdrecht, M. C. M.; Tsuneda, S. Modeling the Nutrient Removal Process in Aerobic Granular Sludge System by Coupling the Reactor- and Granule-Scale Models. *Biotechnol. Bioeng.* **2015**, *112* (1), 53−64.
(35) Brdjanovic, D.; Logemann, S.; van Loosdrecht, M. C. M.; Hooijmans, C. M.; Alaerts, G. J.; Heijnen, J. J. Influence of temperature on biological phosphorus removal: Process and molecular ecological studies. *Water Res.* **1998**, *32* (4), 1035−1048.
(36) Lopez-Vazquez, C. M.; Oehmen, A.; Hooijmans, C. M.; Brdjanovic, D.; Gijzen, H. J.; Yuan, Z. G.; van Loosdrecht, M. C. M. Modeling the PAO-GAO competition: Effects of carbon source, pH and temperature. *Water Res.* **2009**, *43* (2), 450−462.
(37) Volcke, E. I. P.; Picioreanu, C.; De Baets, B.; van Loosdrecht, M. C. M. Effect of granule size on autotrophic nitrogen removal in a granular sludge reactor. *Environ. Technol.* **2010**, *31* (11), 1271−1280.
(38) Reichert, P.; Ruchti, J.; Simon, W. AQUASIM: Computer program for the identification and simulation of aquatic systems. *Hydroinformatics '96*, **1996**, 835−837.
(39) Volcke, E. I. P.; Picioreanu, C.; De Baets, B.; van Loosdrecht, M. C. M. The granule size distribution in an anammox-based granular sludge reactor affects the conversion-Implications for modeling. *Biotechnol. Bioeng.* **2012**, *109* (7), 1629−1636.
(40) Volcke, E. I. P.; Sanchez, O.; Steyer, J. P.; Dabert, P.; Bernet, N. Microbial population dynamics in nitrifying reactors: Experimental evidence explained by a simple model including interspecies competition. *Process Biochem.* **2008**, *43* (12), 1398−1406.
(41) Gieseke, A.; Bjerrum, L.; Wagner, M.; Amann, R. Structure and activity of multiple nitrifying bacterial populations co-existing in a biofilm. *Environ. Microbiol.* **2003**, *5* (5), 355−369.
(42) Blackburne, R.; Vadivelu, V. M.; Yuan, Z. G.; Keller, J. Kinetic characterisation of an enriched Nitrospira culture with comparison to Nitrobacter. *Water Res.* **2007**, *41* (14), 3033−3042.
(43) Kaelin, D.; Manser, R.; Rieger, L.; Eugster, J.; Rottermann, K.; Siegrist, H. Extension of ASM3 for two-step nitrification and denitrification and its calibration and validation with batch tests and pilot scale data. *Water Res.* **2009**, *43* (6), 1680−1692.
(44) Smolders, G. J. F.; Vandermeij, J.; van Loosdrecht, M. C. M.; Heijnen, J. J. A Structured Metabolic Model for Anaerobic and Aerobic Stoichiometry and Kinetics of the Biological Phosphorus Removal Process. *Biotechnol. Bioeng.* **1995**, *47* (3), 277−287.
(45) Zeng, R. J.; Lemaire, R.; Yuan, Z.; Keller, J. Simultaneous nitrification, denitrification, and phosphorus removal in a lab-scale sequencing batch reactor. *Biotechnol. Bioeng.* **2003**, *84* (2), 170−178.
(46) Bassin, J. P.; Kleerebezem, R.; Dezotti, M.; van Loosdrecht, M. C. M. Simultaneous nitrogen and phosphate removal in aerobic granular sludge reactors operated at different temperatures. *Water Res.* **2012**, *46* (12), 3805−3816.
(47) Filipe, C. D. M.; Daigger, G. T.; Grady, C. P. L. A metabolic model for acetate uptake under anaerobic conditions by glycogen accumulating organisms: Stoichiometry, kinetics, and the effect of pH. *Biotechnol. Bioeng.* **2001**, *76* (1), 17−31.
(48) Winkler, M. K. H.; Bassin, J. P.; Kleerebezem, R.; de Bruin, L. M. M.; van den Brand, T. P. H.; van Loosdrecht, M. C. M. Selective sludge removal in a segregated aerobic granular biomass system as a strategy to control PAO-GAO competition at high temperatures. *Water Res.* **2011**, *45* (11), 3291−3299.
(49) Gieseke, A.; Purkhold, U.; Wagner, M.; Amann, R.; Schramm, A. Community structure and activity dynamics of nitrifying bacteria in a phosphate-removing biofilm. *Appl. Environ. Microbiol.* **2001**, *67* (3), 1351−1362.
(50) Dionisi, H. M.; Layton, A. C.; Harms, G.; Gregory, I. R.; Robinson, K. G.; Sayler, G. S. Quantification of Nitrosomonas oligotropha-like ammonia-oxidizing bacteria and Nitrospira spp. from full-scale wastewater treatment plants by competitive PCR. *Appl. Environ. Microbiol.* **2002**, *68* (1), 245−253.
(51) Juretschko, S.; Loy, A.; Lehner, A.; Wagner, M. The microbial community composition of a nitrifying-denitrifying activated sludge from an industrial sewage treatment plant analyzed by the full-cycle rRNA approach. *Syst. Appl. Microbiol.* **2002**, *25* (1), 84−99.
(52) Waltermann, M.; Steinbuchel, A. Neutral lipid bodies in prokaryotes: Recent insights into structure, formation, and relationship to eukaryotic lipid depots. *J. Bacteriol.* **2005**, *187* (11), 3607−3619.
(53) van Loosdrecht, M. C. M.; Pot, M. A.; Heijnen, J. J. Importance of bacterial storage polymers in bioprocesses. *Water Sci. Technol.* **1997**, *35* (1), 41−47.
(54) Blackburne, R.; Vadivelu, V. M.; Yuan, Z. G.; Keller, J. Determination of growth rate and yield of nitrifying bacteria by measuring carbon dioxide uptake rate. *Water Environ. Res.* **2007**, *79* (12), 2437−2445.

DOI: 10.1021/acs.est.5b01952
Environ. Sci. Technol. 2015, 49, 11003−11010